



PAPER • OPEN ACCESS

Dicke time crystals in driven-dissipative quantum many-body systems

To cite this article: Bihui Zhu *et al* 2019 *New J. Phys.* **21** 073028

View the [article online](#) for updates and enhancements.

You may also like

- [Non-stationarity and dissipative time crystals: spectral properties and finite-size effects](#)
Cameron Booker, Berislav Bua and Dieter Jaksch
- [Many-body effects and quantum fluctuations for discrete time crystals in Bose–Einstein condensates](#)
Jia Wang, Peter Hannaford and Bryan J Dalton
- [From a continuous to a discrete time crystal in a dissipative atom-cavity system](#)
Hans Keßler, Jayson G Cosme, Christoph Georges *et al.*



PAPER

Dicke time crystals in driven-dissipative quantum many-body systems

OPEN ACCESS

RECEIVED

1 April 2019

REVISED

8 May 2019

ACCEPTED FOR PUBLICATION

19 June 2019

PUBLISHED

17 July 2019

Original content from this work may be used under the terms of the [Creative Commons Attribution 3.0 licence](#).

Any further distribution of this work must maintain attribution to the author(s) and the title of the work, journal citation and DOI.

**Bihui Zhu**^{1,2}, **Jamir Marino**^{2,3,4}, **Norman Y Yao**^{5,6}, **Mikhail D Lukin**² and **Eugene A Demler**²¹ ITAMP, Harvard-Smithsonian Center for Astrophysics, Cambridge, MA 02138, United States of America² Department of Physics, Harvard University, Cambridge MA 02138, United States of America³ Department of Quantum Matter Physics, University of Geneva, 1211, Geneva, Switzerland⁴ Kavli Institute for Theoretical Physics, University of California, Santa Barbara, CA 93106-4030, United States of America⁵ Department of Physics, University of California, Berkeley, CA 94720, United States of America⁶ Materials Sciences Division, Lawrence Berkeley National Laboratory, Berkeley CA 94720, United States of AmericaE-mail: demler@physics.harvard.edu and bihui.zhu.physics@gmail.com**Keywords:** quantum many-body physics, dynamical phases of matter, driven dissipative systems

Abstract

The Dicke model—a paradigmatic example of superradiance in quantum optics—describes an ensemble of atoms which are collectively coupled to a leaky cavity mode. As a result of the cooperative nature of these interactions, the system’s dynamics is captured by the behavior of a single mean-field, collective spin. In this mean-field limit, it has recently been shown that the interplay between photon losses and periodic driving of light–matter coupling can lead to time-crystalline-like behavior of the collective spin (Gong *et al* 2018 *Phys. Rev. Lett.* **120** 040404). In this work, we investigate whether such a Dicke time crystal (TC) is stable to perturbations that explicitly break the mean-field solvability of the conventional Dicke model. In particular, we consider the addition of short-range interactions between the atoms which breaks the collective coupling and leads to complex many-body dynamics. In this context, the interplay between periodic driving, dissipation and interactions yields a rich set of dynamical responses, including long-lived and metastable Dicke-TCs, where losses can cool down the many-body heating resulting from the continuous pump of energy from the periodic drive. Specifically, when the additional short-range interactions are ferromagnetic, we observe time crystalline behavior at non-perturbative values of the coupling strength, suggesting the possible existence of stable dynamical order in a driven-dissipative quantum many-body system. These findings illustrate the rich nature of novel dynamical responses with many-body character in quantum optics platforms.

1. Introduction

The study of emergent dynamical phenomena in interacting quantum many-body systems constitutes a frontier of research in modern quantum optics and condensed matter physics. In this quest for phases of quantum matter without equilibrium counterpart, time crystals (TCs) represent a promising candidate for a novel form of dynamical order out-of-equilibrium. In TCs, observables dynamically entrain at a frequency subharmonic of the one imposed by an external periodic drive [1–18], and they have been currently realized with trapped ions [19] and solid state systems [20–22]. In most previous studies, TCs are realized in closed interacting quantum many-body systems, which are prone to heating towards an infinite temperature state under the action of periodic drive [23, 24], therefore, a slowdown of energy absorption is customarily entailed via a disorder induced many-body localized phase [25–28], or by fast driving [8, 29–33].

An alternative pathway could consist in ‘cooling’ TC via coupling to a cold bath, which can absorb the energy pumped by the periodic drive [32]. A natural candidate to explore this avenue is represented by a recent line of inquiry on the exploration of TC-like behavior in the open Dicke model, which describes an ensemble of atoms collectively coupled to a leaky photon cavity mode. The periodic drive of Dicke light–matter interactions in the superradiant regime can entail sub-harmonic dynamical responses [1], however, the collective nature of

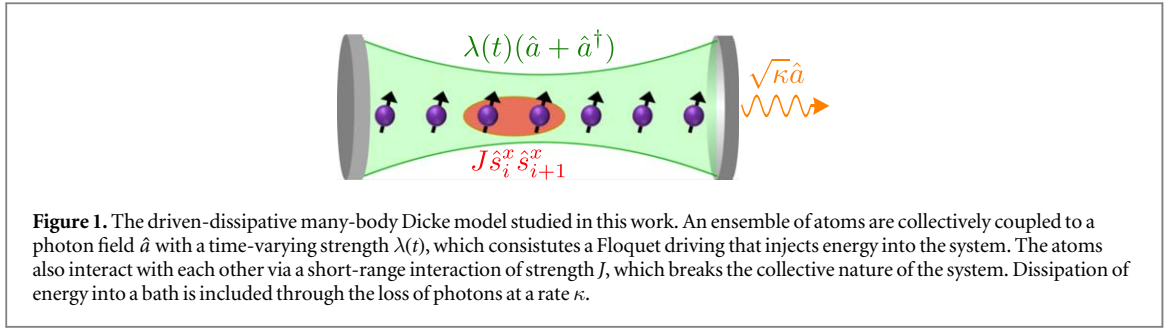


Figure 1. The driven-dissipative many-body Dicke model studied in this work. An ensemble of atoms are collectively coupled to a photon field \hat{a} with a time-varying strength $\lambda(t)$, which constitutes a Floquet driving that injects energy into the system. The atoms also interact with each other via a short-range interaction of strength J , which breaks the collective nature of the system. Dissipation of energy into a bath is included through the loss of photons at a rate κ .

interactions renders the dynamics of this class of TCs equivalent to a single body problem consisting of a mean-field collective spin degree of freedom moving on the Bloch sphere. Our key goal is to understand the stability of the Dicke-TC when one breaks the mean-field nature of the model.

To this end, we explore the robustness of Dicke-TCs to local interactions which break the collective coupling of the original model (figure 1). We observe that this class of Dicke-TCs can remain stable to such mean-field breaking perturbations in certain limits. Crucially, this lifts the phenomenon from an inherently collective, mean-field effect to the steady-state behavior of a dissipative many-body system. We note however, that unlike the traditional venue for discrete TC [9–13], where short-range interactions are essential for *stabilizing* time crystalline order, here, the short-range interactions are rather viewed as *perturbations* to the original mean-field Dicke-TC.

The interplay between Floquet driving, dissipation, and interactions results in a rich set of dynamical responses. In particular, we find regimes where TCs are stabilized by the bath, which counteracts the energy pumped into the system by the drive. We also observe the emergence of metastable dissipative TCs, characterized by a slowly decaying envelope evolving eventually into a trivial steady state dominated by dissipation. In addition, we find a family of ferromagnetic driven-dissipative TCs with strong resilience to many-body heating.

2. The model

We consider a chain of N two-level atoms with short-range interactions among each other

$$\hat{H}_{\text{int}} = J \sum_{i=1}^N \hat{s}_i^x \hat{s}_{i+1}^x, \quad (1)$$

where $\hat{s}^{x,y,z} = \hat{\sigma}^{x,y,z}/2$, and $\hat{\sigma}^{x,y,z}$ are Pauli matrices. The atoms are collectively coupled to a photon field, e.g. by placing them inside an optical cavity (figure 1), which can be described by the Hamiltonian [34, 35]

$$\hat{H}_{\text{ac}} = \omega \hat{a}^\dagger \hat{a} + \omega_0 \hat{S}_z + \frac{2\lambda(t)}{\sqrt{N}} (\hat{a} + \hat{a}^\dagger) \hat{S}_x, \quad (2)$$

where $\hat{S}_{x,y,z} = \sum_i^N \hat{s}_i^{x,y,z}$. We allow the light-matter coupling to be varied in time, $\lambda(t)$. Dissipation occurs when photons leak out of the cavity, as encoded by the quantum master equation

$$\dot{\hat{\rho}} = -i[\hat{H}, \hat{\rho}] + \frac{\kappa}{2} (2\hat{a}\hat{\rho}\hat{a}^\dagger - \hat{a}^\dagger\hat{a}\hat{\rho} - \hat{\rho}\hat{a}^\dagger\hat{a}), \quad (3)$$

for the total density matrix of the system, $\hat{\rho}$, where $\hat{H} = \hat{H}_{\text{ac}} + \hat{H}_{\text{int}}$, and κ characterizes the rate of photon loss.

When $J = 0$, the above reduces to the well-known open Dicke model [36–53]. As the coupling is only between the single photon mode and the collective spin operator, \hat{S}_x , the Dicke model is exactly solvable in the thermodynamic limit $N \rightarrow \infty$: its dynamics can be described by the mean-field motion of the photonic amplitude, $a = \langle \hat{a} \rangle$, coupled to three classical degrees of freedom, $S_{x,y,z}(t) = \langle \hat{S}_{x,y,z}(t) \rangle$, evolving on the Bloch sphere. When $J \neq 0$, short-range atom-atom interactions break the exact solvability of \hat{H}_{ac} , spoiling the collective character of the Dicke Hamiltonian. In addition to the collective mode \vec{S} , which corresponds to the $k = 0$ Fourier mode $\vec{s}_k \equiv \sum_{j=1}^N e^{-ikj} \vec{s}_j$, all other $k \neq 0$ modes could also be excited. Hence \hat{H}_{int} introduces quantum fluctuations in the spin (or atomic) degrees of freedom, which require treating the dynamics in equation (3) as a quantum many-body problem.

We simultaneously account for dissipation and quantum fluctuations using a time-dependent spin-wave approach, which has been demonstrated effective in capturing dynamical quantum many-body effects [54–56]. Specifically, we first perform a time-dependent rotating frame transformation to align the time-dependent

\hat{z} -axis with the collective Bloch vector $\vec{S}(t)$, and then in this co-moving ‘frame’ we perform a Holstein–Primakoff transformation in order to expand the spin operators in \hat{H}_{int} to the lowest-order in the density of spin-wave excitations, $\epsilon(t)$ (see appendix A for details). The many-body effects introduced by \hat{H}_{int} are encoded in the dynamical coupling between spin-waves, and the collective spin as well as photon field. Excitation of spin waves leads to a depletion of the $k = 0$ mode, $2|\vec{S}(t)|/N = 1 - \epsilon(t)$, similarly in spirit to approaches which incorporate self-consistently the effect of quantum fluctuations in the dynamics of a ‘condensate’ [57]. The spin-wave density, $\epsilon(t)$, representing the total population of all $k \neq 0$ spin-wave excitations, is required to remain small at all times in order to have a self-consistent lowest-order Holstein–Primakoff expansion. By monitoring the growth of spin-wave density, we can identify regions of ‘heating’, where the collective spin order shrinks under the effect of strong many-body interactions, accompanied by a large value of $\epsilon(t)$ in dynamics (see appendix A).

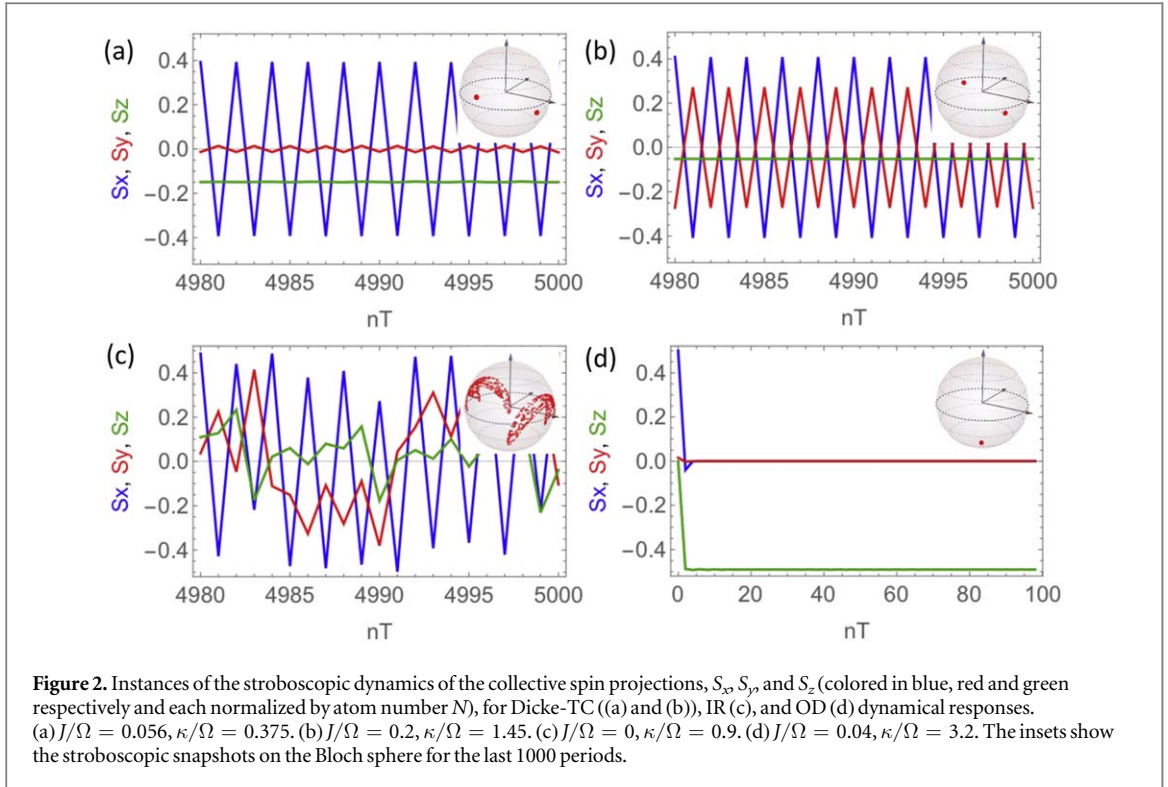
3. Dynamical responses

We impose a periodic modulation on the light–matter coupling $\lambda(t)$: during a first ‘bright-time’, $nT \leq t < (n + 1/2)T$, we set $\lambda(t) = \lambda = \Omega$, and during the ‘dark-time’, $(n + 1/2)T \leq t < nT$, we switch off $\lambda(t)$. Here, $\Omega = 2\pi/T = (\omega_0 + \omega)/2$ denotes the driving frequency. This periodic driving counteracts with the energy loss through photon leaking, and as previously found in [1] for the collective Dicke model (\hat{H}_{int} absent), it entails a period-doubling response in spin observables. The presence of such TC-like behavior can be understood from the \mathbb{Z}_2 symmetry of the Dicke model with constant λ , under the parity operator $P = e^{i\pi(\hat{a}^\dagger \hat{a} + \hat{S}_z + \frac{N}{2})}$. For $\lambda > \lambda_c = \frac{1}{2}\sqrt{(\omega^2 + \kappa^2/4)\omega_0/\omega}$, a quantum phase transition that breaks the \mathbb{Z}_2 symmetry occurs, and the system enters a superradiant phase, featuring two steady states, with spin projection $S_x/N = \pm X$, $S_y = 0$ and non-vanishing photon amplitude $a = \mp\sqrt{N}\lambda X/(\omega - i\kappa/2)$ ($X = \frac{1}{2}\sqrt{1 - \lambda_c^4/\lambda^4}$). When $\delta \equiv (\omega_0 - \omega)/\Omega = 0$, the free evolution during the ‘dark-time’ accumulates a phase of π for both S_x and a , and the system switches from one steady state to another, i.e. $S_x \rightarrow -S_x$ and $a \rightarrow -a$. As a result, the dynamics repeats after two cycles of the driving and a sub-harmonic response with period $2T$ appears. In such a picture, atoms are simply described as a single classical spin, which becomes invalid in the presence of \hat{H}_{int} , and thus it deserves a careful investigation whether the Dicke-TC exists in a many-body system with nonzero J .

We explore the spin dynamics for various interaction strength J and dissipation rate κ , using the time-dependent spin-wave approach. Our analysis shows that the Dicke-TC order can exist beyond the collective case ($J = 0$) and survive many-body interactions. For a range of finite $J/\Omega \ll 1$ and $0 < \kappa/\Omega \lesssim 1$, we observe a stable subharmonic response in $S_x(t)$, as plotted in figure 2(a) for an instance, where the spin-wave density remains small and therefore it is robust to heating (see appendix B). Upon increasing the values of J , the inelastic scattering induced by many-body interactions becomes efficient, provoking a sizeable growth of spin-wave density, which invalidates the lowest-order spin-wave expansion and makes the collective spin, \vec{S} , crumble. In this regime of strong interactions, the system is prone to heating under the action of the Floquet driving (see also⁷). However, as shown in figure 2(b), for moderate strengths of $J/\Omega \lesssim 1$, such effect of heating can still be remediated with sufficient dissipation $\kappa/\Omega \gtrsim 1$ (see also appendices B and D). In this case, strong dissipation acts as a ‘contractor’ for the dynamics, guiding swiftly the system towards the desired non-equilibrium steady state and enables stable oscillations of S_x . Meanwhile, the combination of strong dissipation and driving leads to remarkable disturbance of the spin state within each period, resulting in a larger value of S_y , compared to the Dicke-TC at small κ (see figures 2(a) and (b)). Here, the enhanced fluctuation of photon field associated with strong dissipation can induce large phase noise and destroy the Dicke-TC as well; however, for sufficiently large atom number N , the phase noise can still be suppressed, since the amplitude of photon field scales as $\sim\sqrt{N}$ in the superradiant regime (see appendix A), and thus allows the observation of the Dicke-TC.

While period doubling is a fragile dynamical response in one-particle periodically driven systems, i.e. it disappears as a tiny $\delta \neq 0$ is switched on, the collective ($J = 0$) Dicke-TC is robust in a range of small $\delta \neq 0$, thanks to the macroscopic S_x -order built during the superradiant ‘bright-time’ and thanks to the ‘contractive’ role of dissipation which guides the system towards the desired non-equilibrium steady state. Such robustness to deviations from the $\delta = 0$ limit, persists upon inclusion of many-body interactions, $J \neq 0$ (as an example, $\delta = -0.12$ is used for figure 2). The persistence of many-body Dicke-TCs on timescales much longer than $t_\kappa \sim 1/\kappa$ (see the exemplary dynamics in figure 2(a)), indicates that they represent a long-lived phenomenon, since in the presence of dissipation, relaxation is typically expected to occur on timescales inversely proportional to the system-bath coupling, κ . Indeed, we never observe decay of the Dicke-TC order on the longest timescales

⁷ In this work, we choose as upper threshold for spin wave density the value, $\epsilon = 0.2$, in order to delimit the heating region from the other dynamical responses. This choice is motivated by previous studies in [56].



accessible to our numerical study (e.g. see figure 2(a) and footnote⁸). The existence of Dicke-TC is also insensitive to initial conditions. As we checked in our numerical simulations, similar responses are observed over a wide range of initial conditions (see appendix B).

Here, dissipation is capable of stabilizing rather than destroying the Dicke-TC order in $S_x(t)$ since it acts on the photon mode and therefore collectively on spin order. On the contrary, when local losses are introduced, dissipation is intrusive and detrimental, and it destroys TCs (see for instance [58]). Note that in conventional discrete TCs, instead, the interactions serve to lock single-spin dynamics into a stable subharmonic response that is robust to perturbations or imperfections of the drive [13, 19].

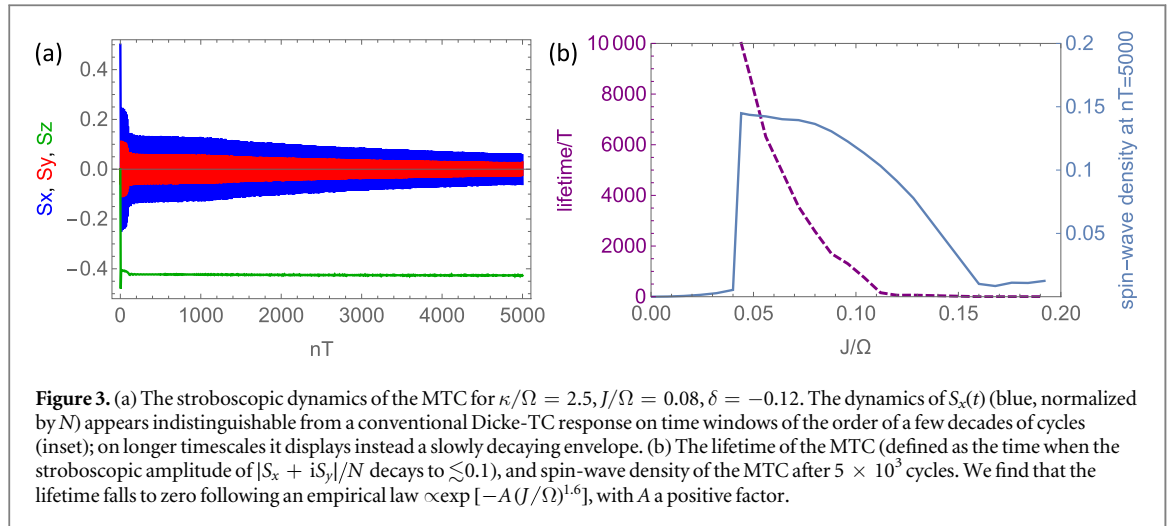
When the rate of dissipation is intermediate, $\kappa/\Omega \sim 1$, we recognize a region of irregular (IR) dynamics, where the trajectory of $\vec{S}(t)$ is scattered on the Bloch sphere (figure 2(c)). In this case, the photon amplitude is sizeably reduced, and since it contributes to building the S_x -order via the light-matter coupling term $\propto \lambda$, the system does not develop a S_x component sufficiently strong in order to counteract the dephasing induced by the ‘transverse field’ $\propto \omega_0 \hat{S}_z$ during the ‘dark-time’, and this results into a featureless dynamical response lacking period-doubling. We also notice that in this regime a relatively small value of J can lead to a proliferation of spin-wave excitations, suggesting a tendency to heating (see appendix D).

Complementarily, with excessively large $\kappa/\Omega \gg 1$, while dissipation is sufficient to cool the system and prevents many-body heating, it also destroys Dicke-TC order: in this case, dissipation overdamps dynamics, and the collective spin of the system relaxes to a trivial steady state where all spins point down towards the south pole of the Bloch sphere (see figure 2(d))⁹. This overdamped (OD) regime is thus characterized by a vanishing magnitude of the spin projection, $|S_x + iS_y|$.

The different dynamical responses discussed above are summarized in a qualitative cartoon, figure D1, in appendix D. It is interesting to note that, with increasing J , we find the system tends to be overdamped with a smaller κ , which is indicated by the downward bending of the boundary between the OD and Dicke-TC regions shown in figure D1. Hence fast ‘cooling’ does not always protect, but can instead destroy Dicke-TC behavior. Nevertheless, dissipation plays a crucial role in establishing the rich phenomena in figure D1 (see appendix E, where the impact of \hat{H}_{int} on TCs in the Lipkin-Meshkov-Glick (LMG) model is addressed). We note that, in this work, the frequency of the drive, Ω , only plays the role of an overall energy scale.

⁸ In principle, we cannot exclude that collapse of the order parameter might occur at much later times, and establishing the stability to infinite times may require another approach, which is beyond the scope of this work. However, this effect, even if present, would be of no practical relevance on experimentally accessible timescales.

⁹ $S_z/N \gtrsim -1/2$, since part of the collective spin is dissipated in the bath of spin waves.



4. Metastable dissipative TC

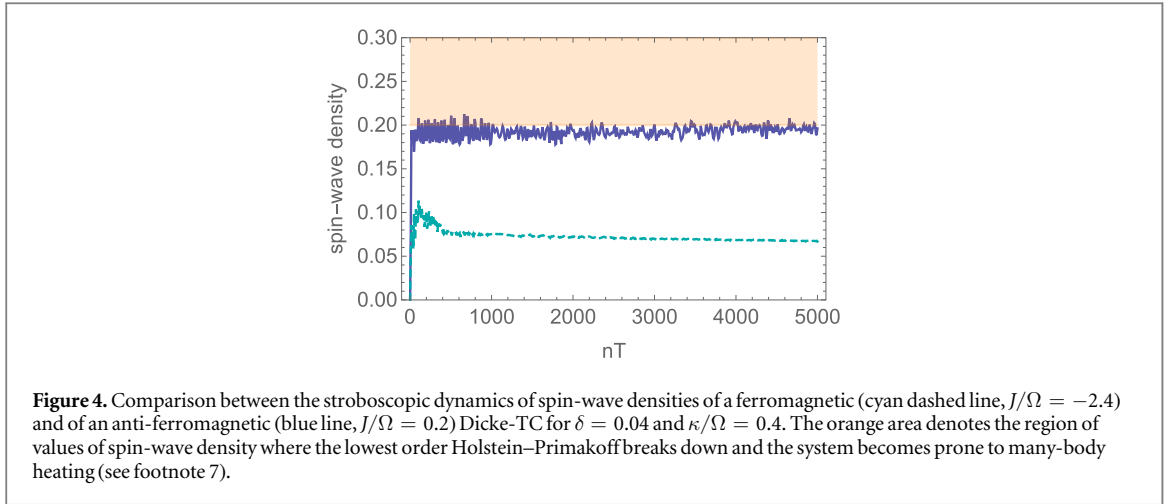
For intermediate values of both J and κ (see for instance figure D1), our system hosts another type of nontrivial behavior: a dissipative metastable time crystal (MTC) characterized by a slowly decaying envelope, which deteriorates, in the long time, into a trivial asymptotic state with vanishing S_x (see figure 3(a)). This behavior is distinct from the Dicke-TC: in figure 3(b) we plot the associated spin-wave density (dark blue line), which exhibits a discontinuous jump at a non-vanishing value of J , when the lifetime of the TC starts also to decrease (purple dashed line); this suggests that the metastability is not expected to manifest for small values of J , and therefore the conventional Dicke-TC represents a long-lived phenomenon (see¹⁰). The lifetime, τ , of this MTC gradually decreases with J , following the empirical law, $\tau \propto \exp[-A(J/\Omega)^{1.6}]$ (with A a positive prefactor), and vanishes when the system enters the OD regime, where also the spin-wave density becomes small since the system reaches the fully polarized state in the negative \hat{z} -direction of the Bloch sphere (corresponding to spin-waves vacuum). The MTC found here appears as a genuine interplay of periodic driving, dissipation and interaction. We remark here that it does not result from a high-frequency expansion [29, 30], and thus is distinct from the ‘prethermal’ Floquet TCs found in previous studies [20, 32], since Ω is an overall energy scale in our system (see figure D1). A possible explanation for the phenomenon is suggested by the dynamics of $\epsilon(t)$: during the metastable evolution, the density of spin waves strongly fluctuates and is out of phase with the dynamics of the photon amplitude, accumulating at every cycle a tiny dephasing, which eventually leads $S_x(t)$ to collapse.

5. Ferromagnetic driven-dissipative TC

As discussed above, the steady state underlying the Dicke-TC order possesses a ferromagnetic nature. When the many-body interaction \hat{H}_{int} is also ferromagnetic ($J < 0$), inter-spin interactions can reinforce the ordering along the $\pm\hat{x}$ -direction, giving rise to robustness against heating and the overdamping caused by dissipation. Indeed, for non-perturbative values of $|J|/\Omega \sim O(1)$, we find that a ferromagnetic ($J < 0$) dissipative Dicke-TC can be stabilized at intermediate dissipation rate without significantly heating up the system (see footnote¹¹). This is shown in figure 4, where we plot the spin-wave density for antiferro- ($J > 0$) and ferro- ($J < 0$) magnetic TCs: a sizeable spin-wave density denotes fragility to many-body interactions and a dynamics prone to heating, and such effects are expected to be pronounced at large J . Remarkably, this does not occur for ferromagnetic inter-spin interactions which develop tiny values of $\epsilon(t)$ even for $|J|/\Omega \sim O(1)$. The emergence of such a Dicke-TC response within the coexistence of significant many-body interactions and dissipation rate, appears to us a strong incarnation of TC-like behavior in driven-dissipative platforms: it is a novel form of dynamical order out-of-equilibrium, which significantly departs both from the mean-field Dicke-TC response (where $J \simeq 0$), and from conventional (many-body) discrete TCs where dissipation is not a constitutive ingredient ($\kappa = 0$). In this perspective, such ferromagnetic TC represents a non-equilibrium state of strongly coupled, driven-dissipative, quantum matter exhibiting rich dynamics that can trigger motivation towards the search of other non-trivial dynamical phases in many-body quantum optics.

¹⁰ We have checked with a finite-size analysis that these conclusions do not depend on N .

¹¹ In this case, we switch off the \hat{H}_{int} term during the ‘dark-time’, in order to avoid inhomogeneous dephasing resulting from inter-spin interactions.



6. Summary and outlook

The Dicke model is currently engineered in several experimental platforms [59–64]. We expect our results to be qualitatively insensitive to the details of the microscopic structure of the interaction term \hat{H}_{int} , and to hold in a broader set of models, and thus would be relevant for experiments where collectivity of the system is inevitably broken by inhomogeneous fields, or spatially varying light–matter couplings, or genuine inter-particle interactions such as using Rydberg atoms [65–68]. The stabilization of Dicke-TC order seen for strong ferromagnetic spin–spin interactions can also be generalized to systems where the inter-spin interactions have an anti-ferromagnetic character ($J > 0$), given the capability to control atom–light coupling in cavity experiments [69]. For coupling $\propto \lambda(\hat{a} + \hat{a}^\dagger)\sum_j (-1)^j \hat{\sigma}_j^x$, a similar Dicke-TC response exists in this case but with anti-ferromagnetic ordering. Hence a \hat{H}_{int} with certain $J > 0$ would be expected to extend the Dicke-TC to a many-body regime. Another interesting possibility offered by the control of light–matter coupling consists in realizing Dicke-TC responses with higher integer periods (nT with $n > 2$) without employing high-spin atoms (see for instance [20]). In the appendix F we show that a Dicke model with coupling of the form $\propto \lambda(\hat{a} + \hat{a}^\dagger)\sum_j [(-1)^{j/2} \hat{\sigma}_j^+ + \text{h.c.}]$ realizes a dynamical response with quadruple period.

The setup analyzed in our work is closely related to quantum optics platform, but can also be relevant for condensed matter and solid state platforms, where the system can be modeled as a quantum spin chain coupled to a phonon bath. We believe that the outreach of our results has the potential to motivate a new generation of experiments on TCs in many-body systems, where the presence of a bath plays a crucial role at variance with current realizations [19, 20].

Acknowledgments

The authors acknowledge discussions with D Abanin, S Gopalakrishnan, W W Ho, R Moessner, C Nayak, V Oganessian, M Schleier-Smith, D Sels and S Yelin. The authors would particularly like to thank F Machado for a careful reading of the draft and many helpful comments. JM acknowledges A Leroze, A Gambassi, A Silva and B Zunkovic for previous collaborations on the subject of time-dependent spin-wave expansions. This work is supported by the DARPA DRINQS program (award D18AC00014, D18AC00033), the NSF (PHY-1748958), the AFOSR-MURI Photonic Quantum Matter (award FA95501610323), the Harvard-MIT CUA, the National Science Foundation (NSF), the David and Lucille Packard Foundation, the W. M. Keck Foundation, and the Vannevar Bush Faculty Fellowship. BZ is supported by the NSF through a grant for the Institute for Theoretical Atomic, Molecular, and Optical Physics at Harvard University and the Smithsonian Astrophysical Observatory. JM is supported by the European Union’s Framework Programme for Research and Innovation Horizon 2020 under the Marie Skłodowska–Curie Grant Agreement No. 745608 (‘QUAKE4PRELIMAT’).

Appendix A. Time-dependent spin-wave theory

In this section we provide further information on the time-dependent spin-wave expansion, referring the reader to [54, 56] for a comprehensive discussion on the method.

We use the shorthand $O \equiv \langle \hat{O} \rangle$ for expectation values of operators \hat{O} , and define the coordinates for the collective spin vector, $\vec{S} = \frac{N}{2}(\sin \theta \cos \phi, \sin \theta \sin \phi, \cos \theta)$, in terms of the polar, θ , and azimuthal angle, ϕ , on the Bloch sphere, which allows writing compactly the equations of motion:

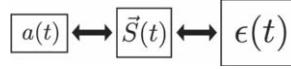


Figure A1. In the time-dependent spin-wave theory, quantum fluctuations introduced by the short-range interaction term \hat{H}_{int} are included as a self-generated bath which couples to the order parameter, $\vec{S}(t)$. The latter couples also to the photonic mode which is cooled by a zero temperature bath. Therefore, the dynamics of the order parameter results from the competing interactions with an internal spin wave bath (represented by spin wave's density, $\epsilon(t)$, in the sketch above), and with an external cold bath, mediated by the cavity photon, $a(t)$.

$$\begin{aligned} \dot{\theta} = & -\frac{2\lambda(t)}{\sqrt{N}}(a + a^*)\sin\phi - J(1 - \epsilon)\sin\theta\sin\phi\cos\phi \\ & + J\delta_{pp}\sin\theta\sin\phi\cos\phi - J\delta_{pq}\sin\theta\cos\theta\cos^2\phi, \end{aligned} \quad (\text{A1a})$$

$$\begin{aligned} \dot{\phi} = & \omega_0 - \frac{2\lambda(t)}{\sqrt{N}}(a + a^*)\cot\theta\cos\phi - J(1 - \epsilon)\cos\theta\cos^2\phi \\ & + J\delta_{qq}\cos\theta\cos^2\phi - 4J\delta_{pq}\sin\phi\cos\phi, \end{aligned} \quad (\text{A1b})$$

$$\dot{a} = -i\omega a - \frac{\kappa}{2}a - i\lambda(t)\sqrt{N}(1 - \epsilon)\sin\theta\cos\phi. \quad (\text{A1c})$$

The effect of \hat{H}_{int} enters the dynamics of the collective spin vector via the spin-wave correlations $\delta_{\alpha\beta}(\alpha, \beta = q, p)$ and the spin-wave density ϵ , which are in turn dynamically coupled to the collective spin and photon field. Here

$$\delta_{\alpha\beta} = \frac{2}{N} \sum_{k \neq 0} \cos k \Delta_k^{\alpha\beta}, \quad \text{and} \quad (\text{A2})$$

$$\epsilon = \frac{1}{N} \sum_{k \neq 0} (\Delta_k^{pp} + \Delta_k^{qq} - 1), \quad (\text{A3})$$

with

$$\Delta_k^{\alpha\alpha} = \langle \hat{\alpha}_k(t) \hat{\alpha}_{-k}(t) \rangle, \quad \text{with } \alpha = q, p, \quad (\text{A4})$$

$$\Delta_k^{pq} = \frac{1}{2} (\langle \hat{p}_k(t) \hat{q}_{-k}(t) \rangle + \langle \hat{q}_k(t) \hat{p}_{-k}(t) \rangle), \quad (\text{A5})$$

where \hat{q}_k and \hat{p}_k are the canonically conjugate bosonic variables associated with spin waves with wave-vector $k \neq 0$.

Following the procedure in [56], we derive the equations of motion for the spin-wave correlations

$$\begin{aligned} \dot{\Delta}_k^{qq} = & -\frac{4\lambda(t)}{\sqrt{N}}(a + a^*)\frac{\cos\phi}{\sin\theta}\Delta_k^{pq} - 2J(\cos^2\phi - \cos k \sin^2\phi)\Delta_k^{pq} \\ & - 2J\cos k \cos\theta \sin\phi \cos\phi \Delta_k^{qq}, \\ \dot{\Delta}_k^{pp} = & \frac{4\lambda(t)}{\sqrt{N}}(a + a^*)\frac{\cos\phi}{\sin\theta}\Delta_k^{pq} + 2J(\cos^2\phi - \cos k \cos^2\theta \cos^2\phi)\Delta_k^{pq} \\ & + 2J\cos k \cos\theta \sin\phi \cos\phi \Delta_k^{pp}, \\ \dot{\Delta}_k^{pq} = & \frac{2\lambda(t)}{\sqrt{N}}(a + a^*)\frac{\cos\phi}{\sin\theta}(\Delta_k^{qq} - \Delta_k^{pp}) + J(\cos^2\phi - \cos k \cos^2\theta \cos^2\phi)\Delta_k^{qq} \\ & - J(\cos^2\phi - \cos k \sin^2\phi)\Delta_k^{pp}. \end{aligned} \quad (\text{A6})$$

These quantities intertwine with the equations of motion (A1), and represent the feedback of the non-equilibrium Gaussian fluctuations of spin waves on the motion of the collective spin (the $k = 0$ mode). The self-consistent solution of equations (A1) and (A6) yields the dynamics of the light–matter system. We note that these equations of motion are derived in the thermodynamic limit [56]; therefore we expect our results to be insensitive to the choice of N , as we checked for the main results of our work.

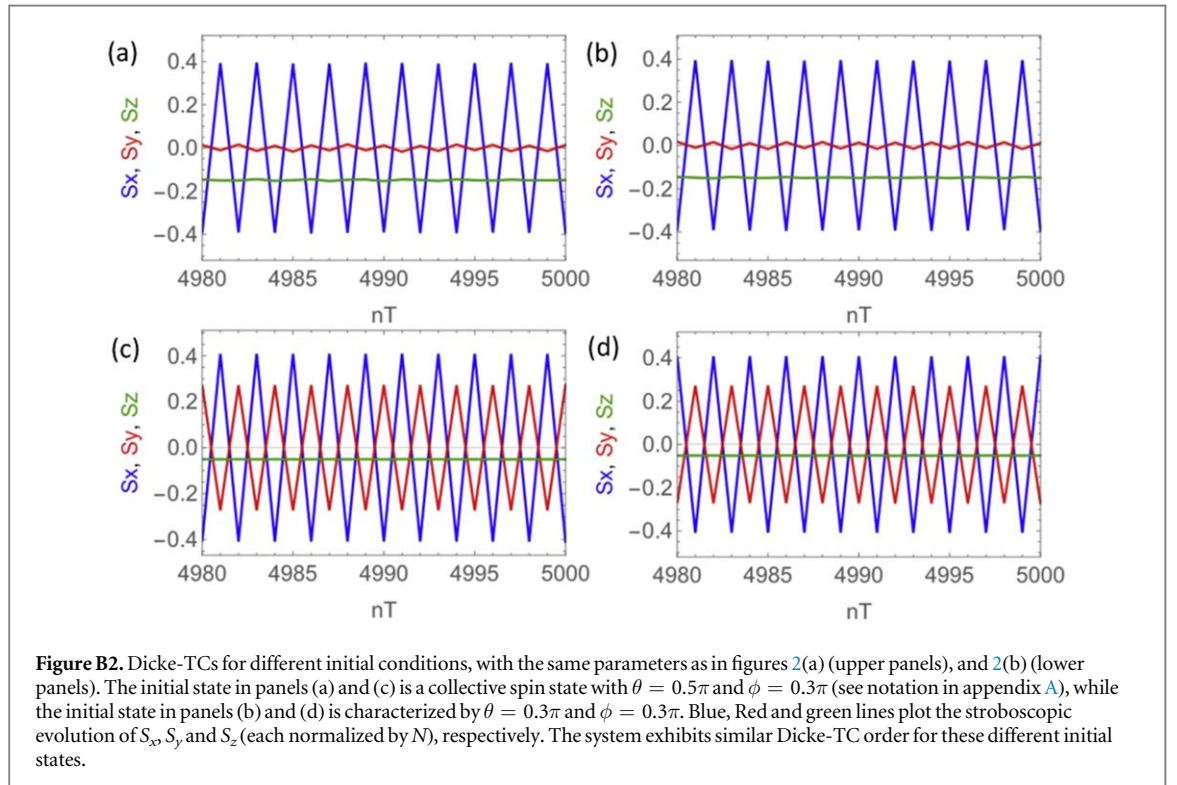
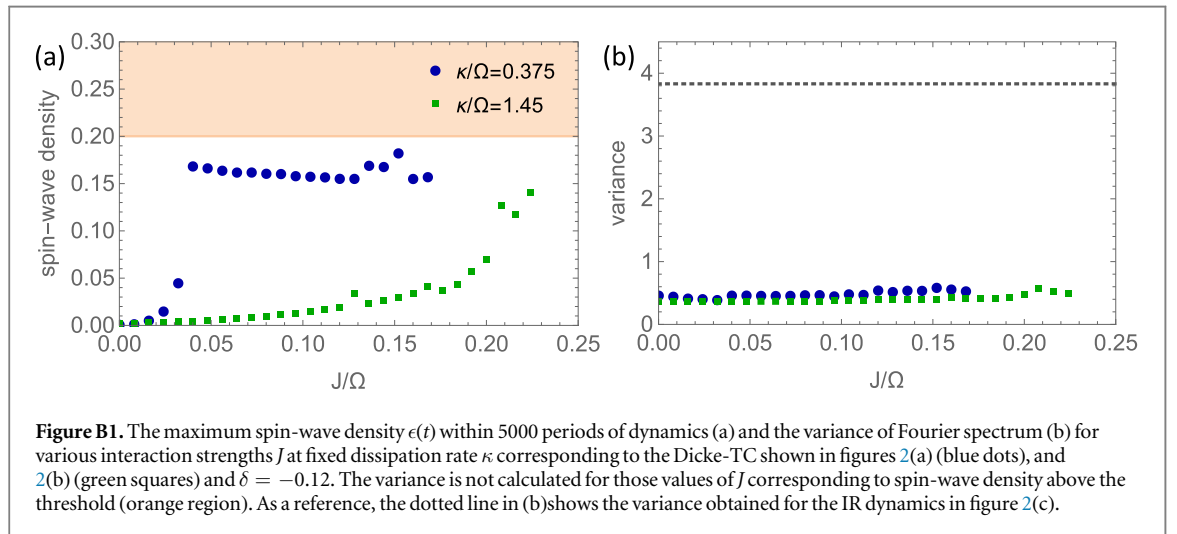
In equation (A1c), the phase fluctuation accompanied with photon loss has been neglected. This is valid in the large N limit, since the TCs under scrutiny here exist in the superradiant regime, where the photon number is $\propto N$, and thus photon noises become subleading. For small N , the effect of phase fluctuation can be incorporated in the spin-wave approach by adding a Langevin noise term in equation (A1c).

To derive equations (A1) and (A6), only terms quadratic in \hat{q}_k , \hat{p}_k have been kept and quartic terms, which scale as ϵ^2 , have been neglected. Hence the spin wave density ϵ has to remain small during the course of the evolution, in order to render consistent the lowest order Holstein–Primakoff expansion. This restriction of the spin-wave approach limits resolving possible structures in the dynamical responses when the heating from J is significant, which might be interesting to explore in future works. For $J = 0$, one can readily see from the above equations that $\epsilon(t) = 0$ at any time, while for $J \neq 0$, the length of the collective spin is shrunk via

$2|\vec{S}(t)|/N = 1 - \epsilon(t)$. A pictorial description of the method is provided in figure A1. The correction from terms higher order than ϵ in the expansion corresponds to interactions between spin-wave excitations and may become quantitatively relevant at long times. As demonstrated in [56], the spin-wave approach can still well capture the dynamics qualitatively even when a sizeable ϵ is developed.

Appendix B. Persistence of Dicke-TC

In this section we provide more details of the Dicke-TC behavior discussed in section 3. In figure B1(a), we plot the maximum spin-wave density over the 5000 periods of dynamics obtained from the above time-dependent spin-wave approach at stroboscopic times, when increasing the interaction strength J . As discussed in the main text, when the system is prone to many-body heating, sizeable amount of spin-waves develops, and the Holstein–Primakoff expansion breaks down. Here, we choose as upper threshold for spin-wave density at the

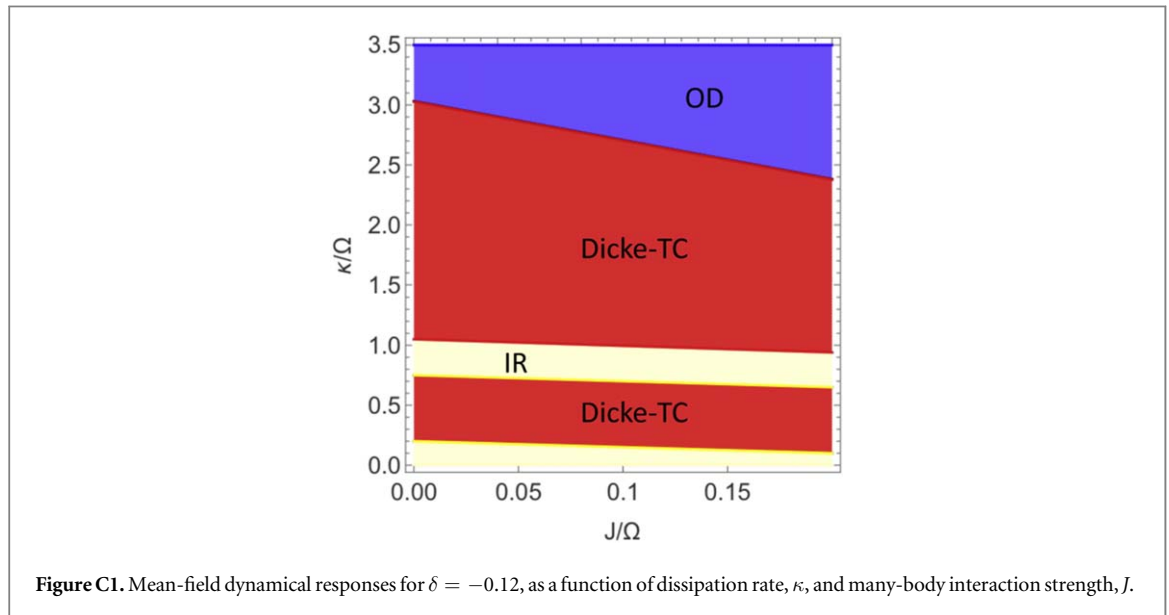


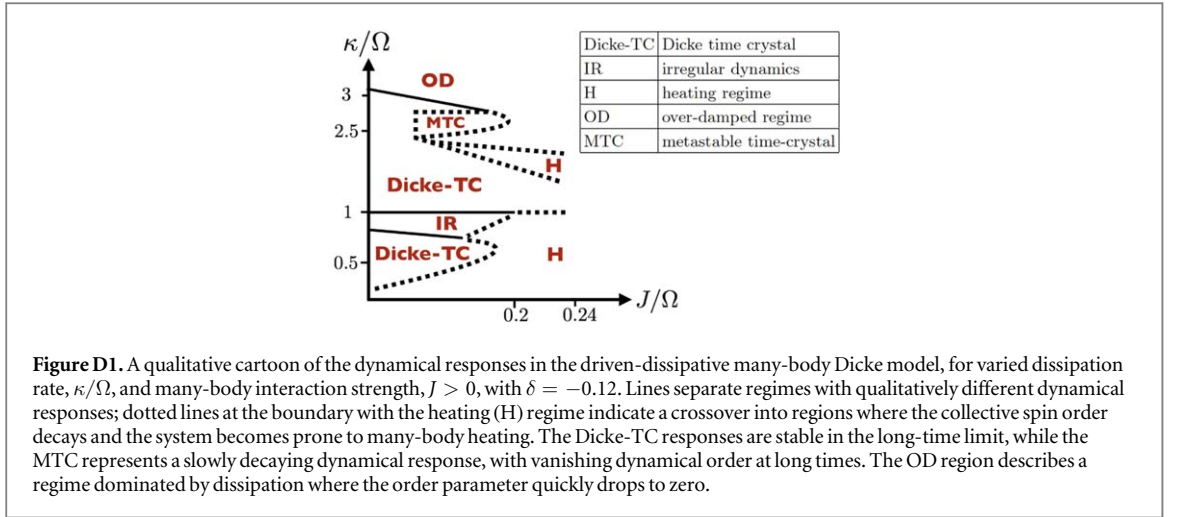
value, $\epsilon = 0.2$. From the spin dynamics, we can also calculate the variance χ of the Fourier spectrum of $S_x + iS_y$, defined as $\chi = \int_{\nu>0} d\nu p(\nu)(\nu - 0.5\Omega) / \int_{\nu>0} d\nu p(\nu) + \int_{\nu<0} d\nu p(\nu)(\nu + 0.5\Omega) / \int_{\nu<0} d\nu p(\nu)$, where $p(\nu)$ is the height of the Fourier spectrum at frequency ν . TCs feature stable subharmonic responses, with the spectrum composed of two sharp peaks located at $\nu = \pm 0.5\Omega$, and thus a small value of χ . The variance for increasing J is plotted in figure B1(b). With a small $\kappa/\Omega < 1$, the spin-wave density quickly grows with J , which is reduced with a large $\kappa/\Omega > 1$. The variance χ remains negligible for values of J with low spin-wave density, indicating the existence of the Dicke-TC with finite J .

In figure 2 an initial state with $\theta = 0.5\pi$ and $\phi = 0$ has been used. We have also checked in our numerical simulations that the Dicke-TC is insensitive to initial conditions, thanks to the dissipative nature of dynamics: we observe similar sub-harmonic dynamics over a wide range of different initial states, as demonstrated in figure B2.

Appendix C. Mean-field analysis of dynamical responses

To understand the dynamical responses in our driven-dissipative many-body system, here, we first apply a mean-field treatment to solve dynamics from the master equation (3). In figure C1 we display the various dynamical responses of the system. The boundaries between the IR and the Dicke-TC regions are dictated by a transition in the variance of the Fourier spectrum of $S_x(t) + iS_y(t)$, which is negligible in the case of the Dicke-TC. The OD regime is identified with a vanishing $|S_x + iS_y|$ at 5000 periods, which exhibits a second-order phase transition when crossing into the Dicke-TC regime. In a mean-field analysis, quantum fluctuations are neglected and thus it does not predict the MTC, the heating region, and the enhanced robustness for ferromagnetic Dicke-TC, which are the genuine many-body results of our study. Instead, it shows as an artifact the persistence of Dicke-TC despite strong interactions.





Appendix D. Summary of dynamical responses from time-dependent spin-wave analysis

To account for quantum many-body effects, we solve equations (A1) and (A6) in the time-dependent spin-wave approach to obtain the spin dynamics. For the numerical integration, we adopt the fourth order Runge–Kutta method and keep a fixed time step of $0.0005T$. We have also checked by halving the time step the conclusions drawn do not change. We explore over a range of parameters κ and J and find rich dynamical responses. Figure D1 shows a qualitative sketch of regions where different dynamical behaviors are observed. We label the region with large spin-wave density $\epsilon(t) \geq 0.2$ as heating (H), where the spin-wave treatment breaks down. IR regime is characterized with a large variance χ of the Fourier spectrum together with $\epsilon(t) < 0.2$. As discussed in [1] for the case of $J = 0$, chaotic dynamics may arise in the collective Dicke model, which can result in large numerical errors. Here, we also find that when $\kappa/\Omega \sim 1$ the numerical integration tends to be unstable, and we associate these instances with IR as well in figure D1. The MTC region is identified with a slow decay of $|S_x + iS_y|$ to a nonzero value at 5000 periods, with a small χ and $\epsilon(t)$ remaining below 0.2. The boundary between the OD and the Dicke-TC regime resembles the one in a mean-field analysis, except that at a small value of J it is interrupted by the emergence of other dynamical behaviors and heating: for increasing J , the boundary is set by a smaller, rather than a larger κ , suggesting that faster dissipation does not always protect the system against the heating from many-body interactions. As noted in appendix A, limited by the choice of truncation in $\epsilon(t)$, a quantitative identification of the parameter regime for all dynamical responses and the nature of their boundaries is beyond the scope of this work.

Appendix E. Comparison with integrability breaking of the periodically kicked LMG model

In order to exemplify the non-trivial interplay that dissipation can have with many-body interactions, we have considered a similar analysis in a case governed by purely unitary dynamics. We have studied the LMG model perturbed by \hat{H}_{int}

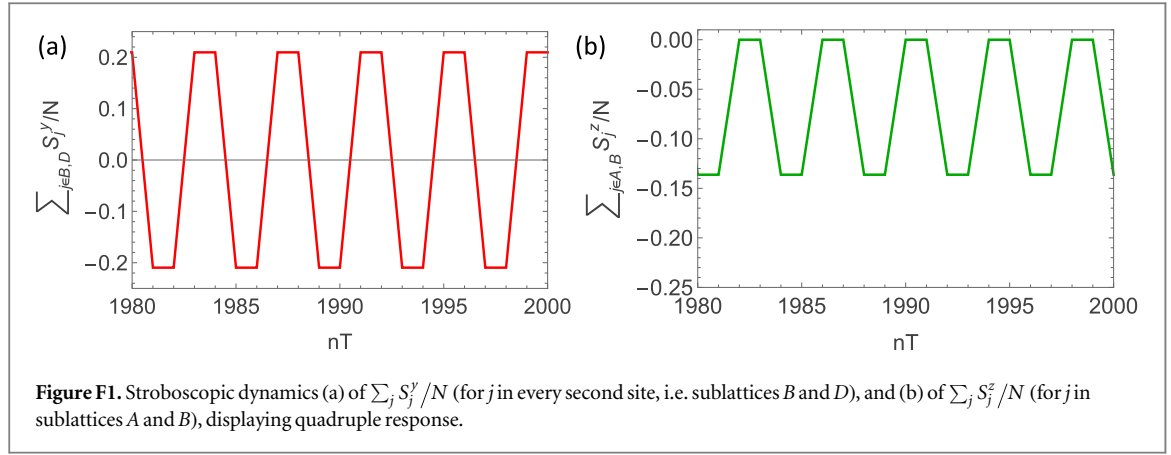
$$\hat{H}' = \hat{H}_{\text{(LMG)}} + \hat{H}_{\text{int}}, \text{ with } \hat{H}_{\text{(LMG)}} = -\frac{\lambda}{N} \hat{S}_x^2 - g \hat{S}_z. \quad (\text{E1})$$

The dynamics entailed by \hat{H}' is periodically perturbed by a collective rotation along the \hat{z} -axis; the evolution operator reads in a period

$$\hat{U} = \hat{U}_{\text{kick}} \exp(-i\hat{H}'T), \quad (\text{E2})$$

with $\hat{U}_{\text{kick}} \equiv \exp(-i\phi \hat{S}_z)$. This protocol has been shown in [70] to display TC behavior when $\phi = \pi$ (in the dynamics of the stroboscopic transverse magnetization). The TC in this case is robust to displacements around the $\phi = \pi$ point, i.e. for angles $\phi = \pi \pm \delta'$ (with $0 < \delta' \ll \pi$). We have chosen this system as a comparison for the Dicke dynamics studied in the main text, since the latter effectively reduces to the LMG model via adiabatic elimination of the photon mode for large cavity detunings.

The periodically driven unitary dynamics in equation (E2) does not entail a rich set of dynamical responses as in figure D1: the TC persists (most likely in a prethermal fashion) for values of J smaller than a certain critical threshold, J_c , above which the system develops sizeable spin-wave density and therefore crosses over into a regime of ‘heating’. This suggests that the presence of dissipation enriches the dynamical responses of a periodically driven interacting quantum many-body system.



Appendix F. Quadruple-period dynamical response

We consider the Hamiltonian

$$\hat{H} = \omega \hat{a}^\dagger \hat{a} + \frac{\omega_0}{2} \sum_j \hat{\sigma}_j^z + \frac{\lambda}{\sqrt{N}} (\hat{a}^\dagger + \hat{a}) \sum_j [e^{ik \cdot \mathbf{x}_j} \hat{\sigma}_j^+ + \text{h.c.}], \quad (\text{F1})$$

with the coupling strength between atoms and cavity controlled by tuning the phase factor $\propto \mathbf{k} \cdot \mathbf{x}_j$. Such coupling can be realized by choosing proper laser dressing in a quantum optics setup. When $e^{ik \cdot \mathbf{x}_j} = 1$, the Hamiltonian (F1) becomes the conventional Dicke model. In the case of $e^{ik \cdot \mathbf{x}_j} \neq 1$, the coupling strength varies from site to site. We choose $e^{ik \cdot \mathbf{x}_j} = (-1)^{j/2}$, therefore, the Hamiltonian becomes

$$\hat{H} = \omega \hat{a}^\dagger \hat{a} + \frac{\omega_0}{2} \sum_j \hat{\sigma}_j^z + \frac{\lambda}{\sqrt{N}} (\hat{a}^\dagger + \hat{a}) \sum_j [\hat{\sigma}_j^x \cos(j\pi/2) - \hat{\sigma}_j^y \sin(j\pi/2)]. \quad (\text{F2})$$

We divide the system into four sublattices, A, B, C and D , with $\text{mod}[j, 4] = \{0, 1, 2, 3\}$, respectively. Within each sublattice, atoms are collectively coupled to cavity photons. In the limit of $N \rightarrow \infty$, the stationary solution of the corresponding master equation hosts multiple possible steady states, depending on the value $Q = \frac{\lambda^2 \omega / \omega_0}{\kappa^2 / 4 + \omega^2}$. The case $Q < 1/4$ corresponds to the normal state without superradiance. When $1/4 \leq Q \leq 1/2$, the system is superradiant, with photon occupation

$$n_{\text{cav}} = \frac{N\omega_0(Q^2 - 1/16)}{\omega Q} \quad (\text{group I}), \quad (\text{F3})$$

and similar to conventional Dicke superradiance, there are two possible spin states:

$$\sigma_A^x = X, \sigma_B^y = -X, \sigma_C^x = -X, \sigma_D^y = X, \quad (\text{F4a})$$

$$\sigma_A^x = -X, \sigma_B^y = X, \sigma_C^x = X, \sigma_D^y = -X, \quad (\text{F4b})$$

with $X = \sqrt{Q^2 - 1/16}/Q$, and both with $\sigma_A^z = \sigma_B^z = \sigma_C^z = \sigma_D^z = -\sqrt{1 - X^2}$. In this case the spin state at each site is in phase with the corresponding photon state. When $Q > 1/2$, the steady state consists of two groups. The first group is the same as in equation (F4), while the photon occupation in the second group is given by

$$n_{\text{cav}} = \frac{N\omega_0(Q^2 - 1/4)}{4\omega Q} \quad (\text{group II}). \quad (\text{F5})$$

This group includes eight different spin configurations

$$\begin{aligned} \sigma_A^x &= X', \sigma_A^z = -Z', \sigma_B^y = X', \sigma_B^z = Z', \sigma_C^x = -X', \\ \sigma_C^z &= -Z', \sigma_D^y = X', \sigma_D^z = -Z', \end{aligned} \quad (\text{F6a})$$

$$\begin{aligned} \sigma_A^x &= X', \sigma_A^z = -Z', \sigma_B^y = -X', \sigma_B^z = -Z', \sigma_C^x = -X', \\ \sigma_C^z &= -Z', \sigma_D^y = -X', \sigma_D^z = Z', \end{aligned} \quad (\text{F6b})$$

$$\begin{aligned} \sigma_A^x &= -X', \sigma_A^z = -Z', \sigma_B^y = X', \sigma_B^z = -Z', \sigma_C^x = X', \\ \sigma_C^z &= -Z', \sigma_D^y = X', \sigma_D^z = Z', \end{aligned} \quad (\text{F6c})$$

$$\begin{aligned} \sigma_A^x &= -X', \sigma_A^z = -Z', \sigma_B^y = -X', \sigma_B^z = Z', \sigma_C^x = X', \\ \sigma_C^z &= -Z', \sigma_D^y = -X', \sigma_D^z = -Z', \end{aligned} \quad (\text{F6d})$$

$$\begin{aligned}\sigma_A^x &= X', \sigma_A^z = Z', \sigma_B^y = X', \sigma_B^z = -Z', \sigma_C^x = X', \\ \sigma_C^z &= -Z', \sigma_D^y = -X', \sigma_D^z = -Z',\end{aligned}\quad (\text{F6e})$$

$$\begin{aligned}\sigma_A^x &= X', \sigma_A^z = -Z', \sigma_B^y = -X', \sigma_B^z = -Z', \sigma_C^x = X', \\ \sigma_C^z &= Z', \sigma_D^y = X', \sigma_D^z = -Z',\end{aligned}\quad (\text{F6f})$$

$$\begin{aligned}\sigma_A^x &= -X', \sigma_A^z = -Z', \sigma_B^y = X', \sigma_B^z = -Z', \sigma_C^x = -X', \\ \sigma_C^z &= Z', \sigma_D^y = -X', \sigma_D^z = -Z',\end{aligned}\quad (\text{F6g})$$

$$\begin{aligned}\sigma_A^x &= -X', \sigma_A^z = Z', \sigma_B^y = -X', \sigma_B^z = -Z', \sigma_C^x = -X', \\ \sigma_C^z &= -Z', \sigma_D^y = X', \sigma_D^z = -Z',\end{aligned}\quad (\text{F6h})$$

with $X' = \sqrt{Q^2 - 1/4}/Q$, and $Z' = \sqrt{1 - X'^2}$. These states correspond to having a ‘defect’ in the spin configurations, and thus result in a lower photon number. A linear stability analysis suggests that the above states can all be stable. The existence of multiple steady states provides the possibility of producing subharmonic responses to external driving.

When $1/4 \leq Q \leq 1/2$, we can have a period-doubled dynamical response if we apply a Floquet driving scheme similar to the one discussed in the main text.

When $Q > 1/2$, in addition to period doubling, we can have a dynamics with period $4T$. However, this would require driving that can convert one steady state to another in equation (F6). A possible procedure is as follows: We initialize spins close to $\sigma_A^x = \sigma_B^y = -\sigma_C^x = \sigma_D^y = 1$, and let the atom-cavity system interact for some time to reach steady state, which can be diagnosed via monitoring the photon emission from cavity. Then we start to apply a driving pulse $\tilde{\theta}$ at the end of each period T . $\tilde{\theta}$ consists of single-site rotations. Specifically, we apply $\hat{R}_z(\pi)$ rotation ($\hat{R}_\alpha(\theta) \equiv \exp(-i\theta\hat{S}_\alpha)$, with $\alpha = x, y, z$) to all odd sites (A and C); even sites (B and D) are rotated depending on the measurement outcome of $\sum_{j \in A} S_j^x$ prior to the pulse: $\hat{R}_z(\pi)$ for negative outcome, and $\hat{R}_y(\pi)$ for positive outcome. The pulse strength is kept equal to cavity detuning.

If we measure $\sum_j S_j^y$ for j in all even sites, we observe a quadruple period in dynamics, as plotted in figure F1, demonstrating that the system indeed undergoes several steady states during the Floquet dynamics. Including small photon loss during $\tilde{\theta}$, we still see oscillations at a stable $4T$ period. An alternative order parameter is the inversion $\sum_j S_j^z$ in sublattices A and B , the dynamics of which also exhibits a period $4T$ (see again figure F1).

The above analysis assumed that atoms within each sublattice remain in the collective manifold and that there are no quantum correlations. When atom number is sufficiently large, this represents a reliable approximation; notice, however, that even for a small number of atoms, period doubling has been observed in [1] to persist for times longer than the decay time, therefore we can expect similar conclusions to hold for the quadruple period dynamics discussed here.

References

- [1] Gong Z, Hamazaki R and Ueda M 2018 *Phys. Rev. Lett.* **120** 040404
- [2] Shapere A and Wilczek F 2012 *Phys. Rev. Lett.* **109** 160402
- [3] Wilczek F 2013 *Phys. Rev. Lett.* **111** 250402
- [4] Bruno P 2013 *Phys. Rev. Lett.* **111** 070402
- [5] Noziers P 2013 *Europhys. Lett.* **103** 57008
- [6] Sacha K 2015 *Phys. Rev. A* **91** 033617
- [7] Watanabe H and Oshikawa M 2015 *Phys. Rev. Lett.* **114** 251603
- [8] Else D V, Bauer B and Nayak C 2016 *Phys. Rev. Lett.* **117** 090402
- [9] Khemani V, Lazarides A, Moessner R and Sondhi S L 2016 *Phys. Rev. Lett.* **116** 250401
- [10] von Keyserlingk C W, Khemani V and Sondhi S L 2016 *Phys. Rev. B* **94** 085112
- [11] von Keyserlingk C W and Sondhi S L 2016 *Phys. Rev. B* **93** 245146
- [12] Khemani V, von Keyserlingk C W and Sondhi S L 2017 *Phys. Rev. B* **96** 115127
- [13] Yao N Y, Potter A C, Potirniche I-D and Vishwanath A 2017 *Phys. Rev. Lett.* **118** 030401
- [14] Yao N, Nayak C, Balents L and Zaletel M 2018 arXiv:1801.02628
- [15] Iemini F, Russomanno A, Keeling J, Schirò M, Dalmonte M and Fazio R 2018 *Phys. Rev. Lett.* **121** 035301
- [16] Tucker K, Zhu B, Lewis-Swan R J, Marino J, Jimenez F, Restrepo J G and Rey A M 2018 *New J. Phys.* **20** 123003
- [17] Gambetta F M, Carollo F, Marcuzzi M, Garrahan J P and Lesanovsky I 2019 *Phys. Rev. Lett.* **122** 015701
- [18] Else D V, Monroe C, Nayak C and Yao N Y 2019 Discrete time crystals arXiv:1905.13232
- [19] Zhang J et al 2017 *Nature* **543** 217
- [20] Choi S et al 2017 *Nature* **543** 221
- [21] Rovny J, Blum R L and Barrett S E 2018 *Phys. Rev. Lett.* **120** 180603
- [22] Rovny J, Blum R L and Barrett S E 2018 *Phys. Rev. B* **97** 184301
- [23] Lazarides A, Das A and Moessner R 2014 *Phys. Rev. E* **90** 012110
- [24] D’Alessio L and Rigol M 2014 *Phys. Rev. X* **4** 041048
- [25] Ponte P, Papić Z, Huveneers F and Abanin D A 2015 *Phys. Rev. Lett.* **114** 140401
- [26] Ponte P, Chandran A, Papić Z and Abanin D A 2015 *Ann. Phys.* **353** 196
- [27] Zhang L, Khemani V and Huse D A 2016 *Phys. Rev. B* **94** 224202
- [28] Bordia P, Lüschen H, Schneider U, Knap M and Bloch I 2017 *Nat. Phys.* **13** 460–4

- [29] Abanin D A, De Roeck W and Huvneers F 2015 *Phys. Rev. Lett.* **115** 256803
- [30] Mori T, Kuwahara T and Saito K 2016 *Phys. Rev. Lett.* **116** 120401
- [31] Ho W W, Choi S, Lukin M D and Abanin D A 2017 *Phys. Rev. Lett.* **119** 010602
- [32] Else D V, Bauer B and Nayak C 2017 *Phys. Rev. X* **7** 011026
- [33] Kuwahara T, Mori T and Saito K 2016 *Ann. Phys.* **367** 96
- [34] Carmichael H, Gardiner C and Walls D 1973 *Phys. Lett. A* **46** 47
- [35] Ritsch H, Domokos P, Brennecke F and Esslinger T 2013 *Rev. Mod. Phys.* **85** 553
- [36] Hepp K and Lieb E H 1973 *Ann. Phys.* **76** 360
- [37] Wang Y K and Hioe F T 1973 *Phys. Rev. A* **7** 831
- [38] Narducci L M, Orszag M and Tuft R A 1973 *Phys. Rev. A* **8** 1892
- [39] Duncan G C 1974 *Phys Rev A* **9** 418
- [40] Garraway B M 2011 *Phil. Trans. R. Soc. A* **396** 1137
- [41] Nagy D, Kónya G, Szirmai G and Domokos P 2010 *Phys. Rev. Lett.* **104** 130401
- [42] Nagy D, Szirmai G and Domokos P 2011 *Phys. Rev. A* **84** 043637
- [43] Keeling J, Bhaseen M J and Simons B D 2010 *Phys. Rev. Lett.* **105** 043001
- [44] Bhaseen M J, Mayoh J, Simons B D and Keeling J 2012 *Phys. Rev. A* **85** 013817
- [45] Dalla Torre E, Diehl S, Lukin M, Sachdev S and Strack P 2013 *Phys. Rev. A* **87** 023831
- [46] Lang J and Piazza F 2016 *Phys. Rev. A* **94** 033628
- [47] Dalla Torre E G, Shchadilova Y, Wilner E Y, Lukin M D and Demler E 2016 *Phys. Rev. A* **94** 061802
- [48] Gelhausen J, Buchhold M and Strack P 2017 *Phys. Rev. A* **95** 063824
- [49] Shchadilova Y, Roses M, Torre E D, Lukin M and Demler E 2018 arXiv:1804.03543
- [50] Drummond P D and Carmichael H J 1978 Volterra cycles and the cooperative fluorescence critical point *Opt. Commun.* **27** 160–4
- [51] Walls D F, Drummond P D, Hassan S S and Carmichael H J 1978 Non-equilibrium phase transitions in cooperative atomic systems *Prog. Theor. Phys.* **64** 307–20
- [52] Kiln S Ya 1982 *JETP* **55** 38
- [53] Kirton P, Roses M M, Keeling J and Dalla Torre E G 2019 Introduction to the Dicke model: from equilibrium to nonequilibrium, and vice versa *Adv. Quantum Technol.* **2** 1800043
- [54] Leroche A, Marino J, Zunkovic B, Gambassi A and Silva A 2018 *Phys. Rev. Lett.* **120** 130603
- [55] Leroche A, Marino J, Gambassi A and Silva A 2018 arXiv:1803.04490
- [56] Leroche A, Zunkovic B, Marino J, Gambassi A and Silva A 2019 *Phys. Rev. B* **99** 045128
- [57] Citro R, Torre E G D, D'Alessio L, Polkovnikov A, Babadi M, Oka T and Demler E 2015 *Ann. Phys.* **360** 694
- [58] Lazarides A and Moessner R 2017 *Phys. Rev. B* **95** 195135
- [59] Black A T, Chan H W and Vuletić V 2003 *Phys. Rev. Lett.* **91** 203001
- [60] Baumann K, Guerlin C, Brennecke F and Esslinger T 2010 *Nature* **464** 1301
- [61] Baumann K, Mottl R, Brennecke F and Esslinger T 2011 *Phys. Rev. Lett.* **107** 140402
- [62] Brennecke F, Mottl R, Baumann K, Landig R, Donner T and Esslinger T 2013 *Proc. Natl Acad. Sci.* **110** 11763
- [63] Klinder J, Keßler H, Bakhtiari M R, Thorwart M and Hemmerich A 2015 *Phys. Rev. Lett.* **115** 230403
- [64] Klinder J, Keßler H, Wolke M, Mathey L and Hemmerich A 2015 *Proc. Natl Acad. Sci.* **112** 3290
- [65] Norcia M A, Lewis-Swan R J, Cline J R K, Zhu B, Rey A M and Thompson J K 2018 *Science* **361** 259
- [66] Vaidya V D, Guo Y, Kroeze R M, Ballantine K E, Kollár A J, Keeling J and Lev B L 2018 *Phys. Rev. X* **8** 011002
- [67] Goban A et al 2014 *Nat. Commun.* **5** 3808
- [68] Epple G, Kleinbach K, Euser T G, Joly N, Pfau T, Russell P S J and Löw R 2014 *Nat. Commun.* **5** 4132
- [69] Kim M E, Chang T H, Fields B M, Chen C-A and Hung C-L 2019 *Nat. Commun.* **10** 1647
- [70] Russomanno A, Iemini F, Dalmonte M and Fazio R 2017 *Phys. Rev. B* **95** 214307